Available online at www.sciencedirect.com
SCIENCE DIRECT®
Journal of Nuclear Materials 352 (2006) 285–290
journal of nuclear materials
www.elsevier.com/locate/jnucmat

Assessment of americium and curium transmutation in magnesia based targets in different spectral zones of an experimental accelerator driven system

W. Haeck [a,b,*], E. Malambu [a], V.P. Sobolev [a], H. Aït Abderrahim [a]

[a] Reactor Physics & MYRRHA Department, Belgian Nuclear Research Centre SCK · CEN, Boeretang 200, B-2400 Mol, Belgium
[b] Ghent University, Subatomic and Radiation Physics, Proeftuinstraat 86, B-9000 Ghent, Belgium

Abstract

The potential to incinerate minor actinides (MA) in a sub-critical accelerator-driven system (ADS) is a subject of study in several countries where nuclear power plants are present. The performance of the MYRRHA experimental ADS, as to the transmutation of Am and Cm in the inert matrix fuel (IMF) samples consisting of 40 vol.% $(Cm_{0.1}Am_{0.5}Pu_{0.4})O_{1.88}$ fuel and 60 vol.% MgO matrix with a density of 6.077 g cm^{-3} in three various spectrum regions, were analysed at the belgian nuclear research centre SCK · CEN. The irradiation period of 810 effective full power days (EFPD) followed by a storage period of 2 years was considered. The ALEPH code system currently under development at SCK · CEN was used to carry out this study. The total amount of MA is shown to decrease in all three considered cases. For Am, the decrease is the largest in the reflector (89% decrease) but at the cost of a net Cm production (92% increase). In the two other positions (inside the core region), 20–30% of Am has disappeared but with a lower production of Cm (between 7% and 11%). In the reflector, a significant build-up of long-lived ^{245}Cm, ^{246}Cm, ^{247}Cm and ^{248}Cm was also observed while the production of these isotopes is 10–1000 times smaller in the core. The reduction of the Pu content is also the highest in the reflector position (41%). In the other positions the incinerated amount of Pu is much smaller: 1–5%.

PACS: 28.41.Bm; 28.41.Kw

1. Introduction

The possibility to incinerate minor actinides (MA) in a sub-critical accelerator-driven system (ADS) is a subject of study in several countries where nuclear power plants are present. The choice of the sub-critical core option and of the cooling technology is among the most important decisions to make. On one side, the fast neutron spectrum is needed for efficient disappearance of MA, because their fission-to-capture ratio is greater at high neutron energies. On the other hand, the sub-criticality allows the loading of MA in a larger fraction of the core that makes the total incineration more efficient than in critical systems.

* Corresponding author. Address: Reactor Physics & MYRRHA Department, Belgian Nuclear Research Centre SCK · CEN, Boeretang 200, B-2400 Mol, Belgium. Tel.: +32 14 33 22 71; fax: +32 14 32 15 29.
E-mail address: whaeck@sckcen.be (W. Haeck).

0022-3115/$ - see front matter © 2006 Elsevier B.V. All rights reserved.
doi:10.1016/j.jnucmat.2006.02.064

Since 1998, the belgian nuclear research centre SCK · CEN is carrying out the design studies aiming at the development of an experimental ADS called MYRRHA (*M*ultipurpose h*y*brid *R*esearch *R*eactor for *H*igh-tech *A*pplication) which could be a step towards a design of a prototype ADS-transmuter [1].

In the present article, the results of evolution of the composition of an inert matrix fuel (IMF) with a high content of americium, curium and low quality (second recycle) plutonium is analyzed during a long-term irradiation in different spectrum regions of the MYRRHA core.

2. Methodology

The transmutation calculations have been performed using the ALEPH code system [2], under development at SCK · CEN in collaboration with Ghent University, which enables us to take into account problem-dependent neutron spectra. This code is designed to be able to use any version of MCNP(X) [3], NJOY 99.90 [4], ORIGEN 2.2 [5] and evaluated nuclear data files (JEF 2.2 was used in this study) in their original ENDF/B-VI format to perform burn-up calculations. At every burn-up step, MCNPX is used to calculate a spectrum in the cells containing material to be burned. These spectra are then used to calculate burn-up dependent one-group cross section libraries for ORIGEN along with the power and/or flux history required for depletion calculations. The microscopic pointwise continuous cross sections used by ALEPH to calculate the one-group cross sections are generated by NJOY. The same nuclear data are used in MCNPX to perform the required core calculations to insure nuclear data consistency.

3. Sub-critical core configuration and irradiation conditions

The MYRRHA ADS concept is based on the coupling of a 5 mA and 350 MeV proton linear accelerator with a liquid lead–bismuth eutectic (LBE) spallation target surrounded by a sub-critical neutron-multiplying core operating at a thermal power of about 50 MW. In order to obtain the fast neutron spectrum, the core is cooled by LBE. $(Pu,U)O_2$ MOX fuel with 30 wt% of Pu in heavy metal made of plutonium from the reprocessed UO_2 light water reactor fuel is used as the driver fuel.

This core consists of a lattice of hexagonal channels loaded with 45 driver fuel assemblies (see Fig. 1), each with 91 fuel pins of 6.55 mm in diameter arranged in a triangular type lattice with a pitch of 8.55 mm ('center-to-center') and an active fuel length of 600 mm. The cladding is made of T91 martensitic steel. The driver MOX fuel pellets in the rods have the initial density of 10.55 g cm^{-3}

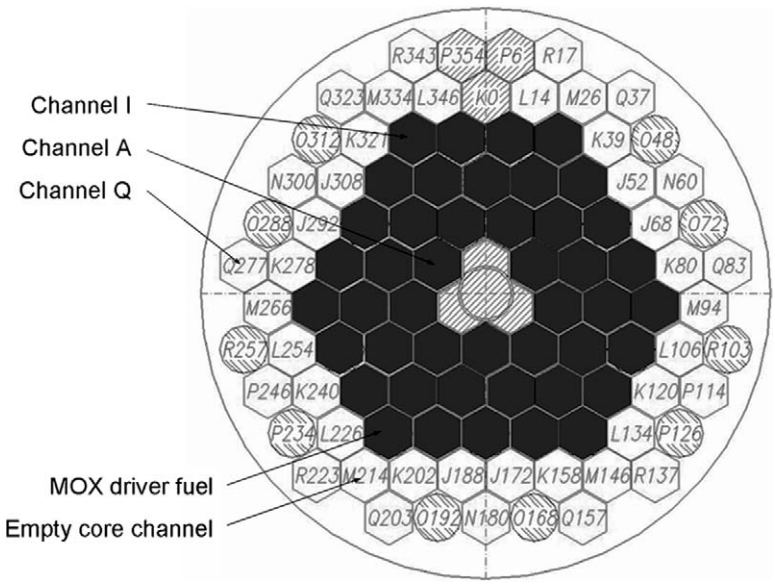

Fig. 1. MYRRHA core configuration and core channel names.

Table 1
Composition of the driver MOX fuel and IMF samples

Fuel type	Isotopic vector	Weight fraction (%)
MOX	U/Pu/O	61.77/26.47/11.76
	$^{234}U/^{235}U/^{236}U/^{238}U$	0.003/0.404/0.10/99.583
	$^{238}Pu/^{239}Pu/^{240}Pu/^{241}Pu/^{242}Pu$	1.27/61.88/23.50/8.95/4.40
IMF	Pu/Am/Cm/Mg/O	24.25/30.32/6.06/19.18/20.19
	$^{238}Pu/^{239}Pu/^{240}Pu/^{241}Pu/^{242}Pu$	5.06/37.91/30.31/13.21/13.51
	$^{241}Am/^{243}Am$	66.67/33.33
	$^{244}Cm/^{245}Cm$	90/10

(~95% TD), and each fresh assembly contains 11.425 kg of heavy metal (~617 kg is the total core load).

The IMF samples to be considered in this report consist of 40 vol.% $(Cm_{0.1}Am_{0.5}Pu_{0.4})O_{1.88}$ fuel and 60 vol.% MgO matrix. The density of the IMF samples is 6.077 g cm^{-3} (~90% TD) with 1.206 g cm^{-3} low quality Pu (second recycle MOX fuel) and 1.809 g cm^{-3} of MA (Cm and Am). The initial isotopic vectors of the MOX and of the IMF samples used in the calculations are given in Table 1 [6,7]. The performance of Am and Cm transmutation has been studied in three positions: channel A (next to the spallation target), channel I (at the periphery of the active core) and channel Q (in the reflector) – see Fig. 1.

For the transmutation calculations described in this paper, the irradiation history consisted of a 3-years campaign of 9 cycles of 90 effective full power days (for a total of 1170 days with 810 EFPD) with 30- or 90-days periods in between for maintenance and core reloading was considered. A 2-years storage (decay and cool-down) period of the spent fuel has also been simulated at the end of the irradiation campaign.

In this exercise, it was assumed that only the IMF targets were irradiated. The spectrum of a full assembly with the targets is similar to that of a MOX fuel assembly in the same position [8] so that we can use the MOX fuel spectrum for the MA samples in channels A and I. We use the unperturbed neutron spectra in channel Q because the samples are small enough so that their influence on the global spectrum will be negligible. The regime of the ADS operation at a constant neutron flux has been considered in order to simplify the calculations. In this case, the loss of core reactivity within a cycle is assumed to be compensated by an increase in the proton beam current and by core reloading.

4. Results and discussion

4.1. Spectra and flux levels

The neutronic parameters of the core have been calculated with MCNPX 2.5.e within the ALEPH code system. The average neutron spectra in the IMF pellets in channels A, I and Q are shown in Fig. 2, where the normalized relative neutron flux per unit of lethargy (the natural logarithm of the ratio of the maximum energy to the neutron energy E) is presented as function of the neutron energy. This representation allows for easy comparison of neutron spectra. The total neutron flux in the channels A, I and Q was calculated to be 3.17×10^{15}, 1.82×10^{15} and 8.88×10^{14} cm^{-2} s^{-1}, respectively.

The spectra for channels A and I are very similar between 1 keV and 10 MeV. Above 10 MeV we can see the high energy tail caused by high energy spallation neutrons in the spectrum of channel A. This high energy tail becomes negligible in the spectra of the two other positions because of a larger distance from the spallation target. In the case of channel Q (the reflector channel), the spectrum is dominated by epithermal neutrons. The number of high energy neutrons (above 1 MeV) is at least 10 times smaller than those for channels A and I. The number of neutrons below 10 keV on the other hand is between 10 and 100 times larger than those in channels A and I. As a result, the incineration performance in channels A and I can be similar. It will, however, be very different from that in channel Q.

4.2. Transmutation performance

Fig. 3 gives the time-evolution of the mass (in gram atom cm^{-3}) for the three actinide elements (Pu, Am, Cm) in the IMF samples over the considered irradiation period. Table 2 gives the mass

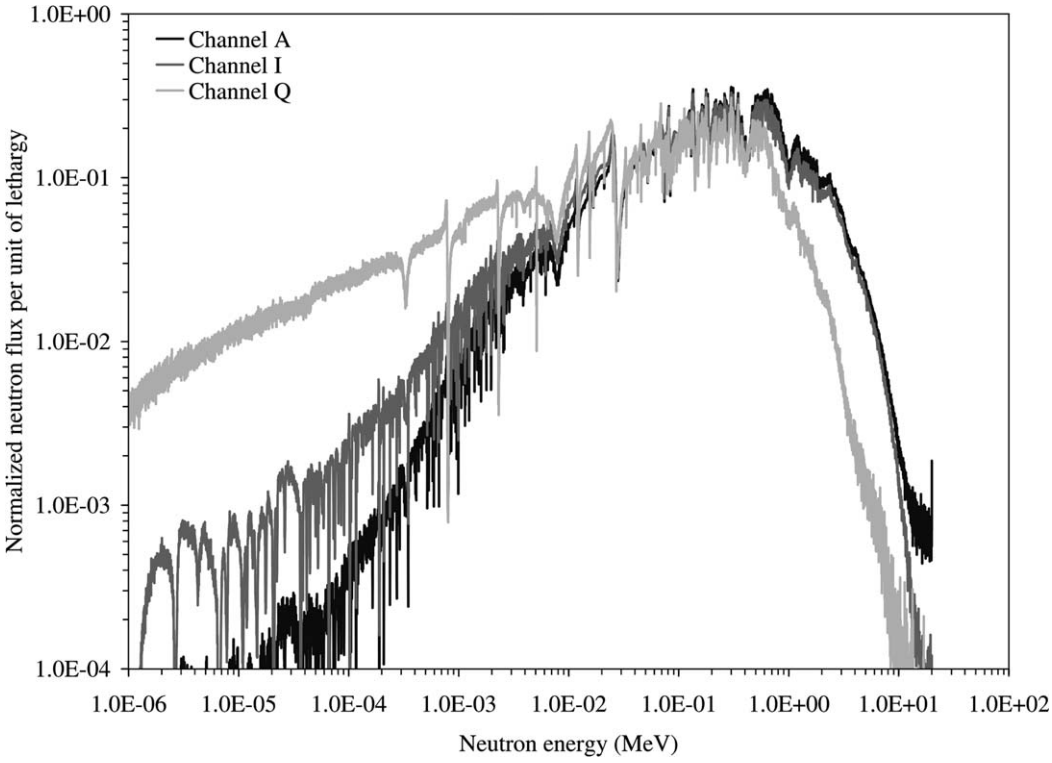

Fig. 2. Normalised neutron spectra near the spallation target (channel A), on the outside of the core (channel I) and in the LBE reflector (channel Q) of the MYRRHA core.

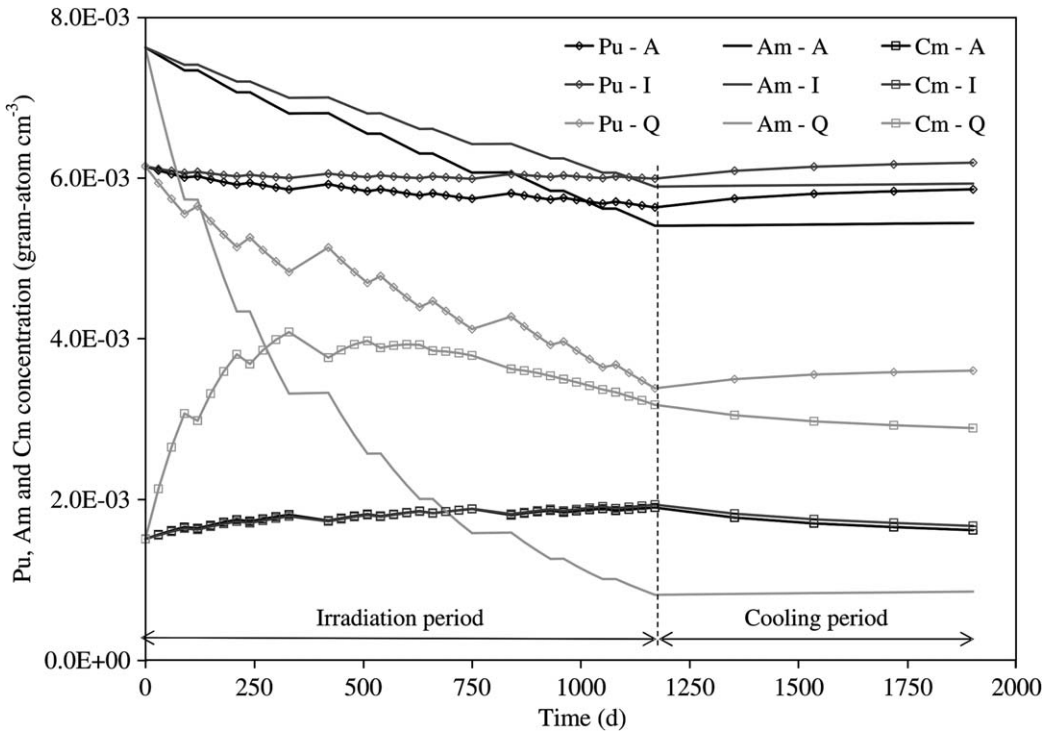

Fig. 3. Evolution of the Pu, Am and Cm concentration in the IMF samples in channels A, I and Q.

Table 2
IMF samples – Pu, Am and Cm mass balance (gram-atom cm^{-3}) for an irradiation period of 1170 days and after cooling near the spallation target (channel A), on the outside of the core (channel I) and in the LBE reflector (channel Q)

Channel		A		I		Q	
Time (d)	0	1170	1900	1170	1900	1170	1900
^{238}Pu	3.13×10^{-4}	8.58×10^{-4}	1.01×10^{-3}	8.19×10^{-4}	9.56×10^{-4}	1.85×10^{-3}	2.01×10^{-3}
^{239}Pu	2.34×10^{-3}	1.50×10^{-3}	1.50×10^{-3}	1.73×10^{-3}	1.73×10^{-3}	5.30×10^{-4}	5.32×10^{-4}
^{240}Pu	1.86×10^{-3}	1.82×10^{-3}	1.94×10^{-3}	1.92×10^{-3}	2.04×10^{-3}	8.28×10^{-5}	1.86×10^{-4}
^{241}Pu	8.08×10^{-4}	5.03×10^{-4}	4.57×10^{-4}	5.74×10^{-4}	5.21×10^{-4}	4.50×10^{-4}	4.08×10^{-4}
^{242}Pu	8.23×10^{-4}	9.49×10^{-4}	9.50×10^{-4}	9.41×10^{-4}	9.42×10^{-4}	4.68×10^{-4}	4.68×10^{-4}
Pu	6.14×10^{-3}	5.63×10^{-3}	5.86×10^{-3}	5.99×10^{-3}	6.19×10^{-3}	3.38×10^{-3}	3.60×10^{-3}
^{241}Am	5.10×10^{-3}	3.37×10^{-3}	3.41×10^{-3}	3.77×10^{-3}	3.81×10^{-3}	2.50×10^{-4}	2.90×10^{-4}
^{242m}Am	–	2.04×10^{-4}	2.03×10^{-4}	1.89×10^{-4}	1.87×10^{-4}	5.45×10^{-5}	5.40×10^{-5}
^{242}Am	–	1.14×10^{-6}	2.42×10^{-9}	1.02×10^{-6}	2.24×10^{-9}	7.45×10^{-7}	6.46×10^{-10}
^{243}Am	2.53×10^{-3}	1.83×10^{-3}	1.83×10^{-3}	1.94×10^{-3}	1.94×10^{-3}	5.10×10^{-4}	5.10×10^{-4}
Am	7.62×10^{-3}	5.41×10^{-3}	5.44×10^{-3}	5.89×10^{-3}	5.93×10^{-3}	8.15×10^{-4}	8.54×10^{-4}
^{242}Cm	–	1.77×10^{-4}	8.48×10^{-6}	1.57×10^{-4}	7.54×10^{-6}	1.94×10^{-4}	8.88×10^{-6}
^{243}Cm	–	9.53×10^{-6}	9.08×10^{-6}	7.63×10^{-6}	7.26×10^{-6}	3.75×10^{-5}	3.58×10^{-5}
^{244}Cm	1.36×10^{-3}	1.51×10^{-3}	1.40×10^{-3}	1.55×10^{-3}	1.44×10^{-3}	1.40×10^{-3}	1.30×10^{-3}
^{245}Cm	1.50×10^{-4}	1.95×10^{-4}	1.95×10^{-4}	2.13×10^{-4}	2.13×10^{-4}	1.16×10^{-3}	1.16×10^{-3}
^{246}Cm	–	9.43×10^{-6}	9.42×10^{-6}	8.72×10^{-6}	8.72×10^{-6}	3.41×10^{-4}	3.41×10^{-4}
^{247}Cm	–	1.61×10^{-7}	1.61×10^{-7}	1.39×10^{-7}	1.39×10^{-7}	3.49×10^{-5}	3.49×10^{-5}
^{248}Cm	–	3.02×10^{-9}	3.02×10^{-9}	2.17×10^{-9}	2.17×10^{-9}	6.52×10^{-6}	6.52×10^{-6}
Cm	1.51×10^{-3}	1.90×10^{-3}	1.62×10^{-3}	1.94×10^{-3}	1.67×10^{-3}	3.18×10^{-3}	2.89×10^{-3}
Total	1.53×10^{-2}	1.29×10^{-2}	1.29×10^{-2}	1.38×10^{-2}	1.38×10^{-2}	7.38×10^{-3}	7.34×10^{-3}

balance of these isotopes for every channel considered before the start of the irradiation, at the end of the irradiation and after the storage period.

During the irradiation periods, the amount of americium in the IMF samples is reduced continuously while it changes weakly during the shutdown and storage periods. As it was expected, the evolution of the Am composition is similar for channels A and I. The fission to capture ratio for these channels are 0.211 and 0.146 at the beginning of the irradiation and 0.281 and 0.187 at the end of the last cycle. Fission accounts for about 20% of all interactions with Am in channel A and for 12–15% of all interactions in channel I. In total, 29% of all Am disappears in the sample in channel A and 22% in channel I.

In the case of channel Q, the amount of Am is reduced more significantly (89% of the Am disappears) mainly due to the large thermal component in the neutron spectrum of this channel. This leads to a lower fission to capture ratio (0.005 at the beginning and 0.103 at the end of the last cycle). Neutron capture is obviously the dominant mechanism for Am transmutation in this channel, as only 0.5% of all interactions at the beginning of the irradiation are fission events (at the end of the last cycle, 10% of all neutron interactions with Am are fissions). The capture cross section of Am in this case is 30 times higher than the capture cross section in channels A and I, while the fission cross section remains roughly the same.

The Am isotopes that have captured a neutron will undergo β-decay and are then converted into Cm. The generated Cm will undergo α-decay and yield Pu [8,9]:

$$^{241}\mathrm{Am} + n \rightarrow {}^{242}\mathrm{Am}(90\%) \overset{(\tau=16\ h)}{\rightarrow} \beta^- + {}^{242}\mathrm{Cm} \overset{(\tau=162\ d)}{\rightarrow} \alpha + {}^{238}\mathrm{Pu}$$
$$\rightarrow {}^{242m}\mathrm{Am}(10\%) \overset{(\tau=141y)}{\rightarrow} \beta^- + {}^{242}\mathrm{Cm} \overset{(\tau=162\ d)}{\rightarrow} \alpha + {}^{238}\mathrm{Pu} \quad (1)$$

$$^{243}\mathrm{Am} + n \rightarrow {}^{244}\mathrm{Am} \overset{(\tau=10.1\ h)}{\rightarrow} \beta^- + {}^{244}\mathrm{Cm} \overset{(\tau=18.1y)}{\rightarrow} \alpha + {}^{240}\mathrm{Pu} \quad (2)$$

The fact that the half-life of ^{242}Am and ^{244}Am is significantly shorter than that of ^{242}Cm and ^{244}Cm respectively and the fact that the capture cross section of Am in channel Q is very high (compared to channels A and I) and that the fission to capture ratio is very low, explains a rapid build-up of Cm in the IMF sample in channel Q during the first few cycles. We can observe an increase of more than 200% of Cm at the end of the third cycle. At that point, already 50% of the total Am content has disappeared. From that point on, the production of Cm is lower than the

Cm disappearance so that the Cm content starts to decrease slowly. At the end of the last cycle, a net production of 110.8% was observed. After the 2-years storage period, this has decreased to 91.6%.

There is also a slight Cm build up during the entire irradiation period in the samples in channels A and I but it is rather small because of the lower capture cross section of Am. In these channels, however, we do not observe a decrease in the Cm build up, except during the storage period where Cm starts to decay. We observe a net production of Cm at the end of the last cycle of 26.0% in channel A and 28.4% in channel I. At the end of the storage period, this has decreased to 7.4% and 10.9%, respectively.

When we look at the individual Cm isotopes, we also observe a drastic build-up of long-lived ^{245}Cm ($T_{1/2} = 8500$ years), ^{246}Cm ($T_{1/2} = 4730$ years), ^{247}Cm ($T_{1/2} = 1.56 \times 10^7$ years) and ^{248}Cm ($T_{1/2} = 3.40 \times 10^5$ years) in channel Q. The production of these isotopes in channels A and I is 10–1000 times lower.

During the shutdown and storage periods the accumulated Cm continues to decay. The decay of ^{242}Cm and ^{244}Cm produces the fertile plutonium isotopes ^{238}Pu and ^{240}Pu. This results in an increase in the total plutonium content during shutdown and storage. ^{238}Pu is also produced during the irradiation by the (n, 2n) reaction in ^{239}Pu. During the irradiation the Pu mass decrease occurs mainly due to fission of the fissile isotopes ^{239}Pu and ^{241}Pu. This explains why the Pu content decreases so rapidly in channel Q (the fission cross section in this channel is about 20 times larger than in channels A and I). We observe a net Pu decrease at the end of the last cycle of 8.3% in channel A, 2.5% in channel I and 44.9% in channel Q. During the storage period this decrease is reduced to 4.7%, 0.7% and 41.4%, respectively.

In total, 15.5% of the MA and Pu in the sample were fissioned or transmuted in channel A, 9.7% in channel I and 51.9% in channel Q. The amount of the disappeared MA is higher in channel Q, but at the cost of a higher increase in Cm content. This is due to the more thermal spectrum in channel Q, which fits, in general, with results published earlier by Berthou et al. [10].

5. Conclusions

The transmutation performance of the MYRRHA ADS using small MA targets in three distinct positions of the core: near the spallation target, on the outside of the core and in the LBE reflector, were modelled. In all three studied cases the total amount of MA is shown to decrease. For Am, the decrease is the highest for the sample in the reflector (89% decrease) but at the cost of a net Cm production (92% increase). In the two other positions, 20–30% of the initial Am mass is incinerated but with a smaller Cm build up (7–11%). In the reflector, we also observe a significant build-up of long-lived ^{245}Cm, ^{246}Cm, ^{247}Cm and ^{248}Cm while the production of these isotopes is 10–1000 times smaller in the core positions. The utilized amount of Pu is also more pronounced in the reflector sample (41%). In the other positions the amount of Pu was reduced only for 1–5%.

Acknowledgement

This work was supported by the funds of the SCK · CEN MYRRHA project.

References

[1] H. Aït Abderrahim, P. Kupschus, E. Malambu, Ph. Benoit, K. Van Tichelen, B. Arien, F. Vermeersch, Y. Jongen, S. Ternier, D. Vandeplassche, Nucl. Instrum. Meth. Phys. Res. A 463 (2001) 487.
[2] W. Haeck, B. Verboomen, H. Aït Abderrahim, C. Wagemans, ALEPH: An efficient approach to Monte Carlo Burnup, Proceeding Am. Nuc. Soc. Topical Meeting on Monte Carlo, Chattanooga, Tennessee, USA, April 17–21, 2005.
[3] J.S. Hendricks, MCNPX-VERSION 2.5.e, LA-UR-04-0569, Technical Report, Los Alamos National Laboratory, USA, 2004.
[4] R.E. MacFarlane, D.W. Muir, The NJOY Nuclear Data Processing System Version 91, Technical Report, LA-12470-M, Los Alamos National Laboratory, USA, 1994.
[5] A.G. Croff, A User's Manual for the ORIGEN2 Computer Code, Technical Report, ORNL/TM-7175, Oak Ridge National Laboratory, USA, 1980.
[6] W.S. Yang, Ann. Nucl. Energy 29 (2002) 509.
[7] W. Maschek, Safety Analyses for Accelerator Driven Transmuters (ADTs) with CERCER and CERMET Fuels, DEL-2 Report, EURATOM FP5 FUTURE project, August 2004.
[8] E. Malambu, W. Haeck, V. Sobolev, H. Aït Abderrahim, MA and LLFP Transmutation Performance Assessment in the MYRRHA small-scale ADS, Proceeding of 8th International Exchange Meeting on P&T, Las Vegas, Nevada, USA, November 8–11, 2004.
[9] W. Seelmann-Eggebert, Karlsruhe Nuklidekarte, KfK, Karlsruhe, 5. Auflage, 1981.
[10] V. Berthou, C. Degueldre, J. Magill, J. Nucl. Mater. 320 (2003) 156.